Research, Ono Medical Research Foundation, Yokoyama Foundation for Clinical Pharmacology, and The Uehara Memorial Foundation. Michiko Itoh was supported by Research Fellowship of Japan Society for the Promotion of Science. Co-author Hiroyuki Kawano is employed by Mochida Pharmaceutical Co. Ltd. Mochida Pharmaceutical Co. Ltd. provided support in the form of salary for Hiroyuki Kawano, but did not have any additional role in the study design, data collection and analysis, decision to publish, or preparation of the manuscript. The specific role of this author is articulated in the 'author contributions' section.

**Competing Interests:** Hiroyuki Kawano is an employee of Mochida Pharmaceutical Co. Ltd., which funded this study and provided highly purified EPA ethyl ester. There are no other potential conflicts of interest relevant to this article. This does not alter the authors' adherence to PLOS ONE policies on sharing data and materials.

## Introduction

Non-alcoholic fatty liver disease (NAFLD) is recognized as a hepatic phenotype of the metabolic syndrome [1]. It encompasses a wide spectrum of liver impairment ranging from benign simple steatosis to non-alcoholic steatohepatitis (NASH), which can lead to cirrhosis and hepatocellular carcinoma [1]. The "two-hit" hypothesis has been proposed as a potential mechanism underlying NASH, in which the first step involves the excessive accumulation of lipids in the liver, thereby sensitizing the liver to the second hits including oxidative stress, lipopolysaccharide, proinflammatory cytokines and adipocytokines [2–4]. However, the precise mechanisms involved in the disease progression from simple steatosis to NASH and hepatocellular carcinoma are still unclear. Accordingly, specific and definitive therapeutic strategies against NASH have not been fully established. It is partly because there are few animal models that reflect the pathophysiology of human NASH.

Recently, we have reported that melanocortin 4 receptor-deficient (MC4R-KO) mice fed high-fat diet develop a liver condition similar to human NASH, which is associated with obesity, insulin resistance and dyslipidemia [5]. MC4R is a seven-transmembrane G protein-coupled receptor that is implicated in the regulation of food intake and body weight [6]. Because MC4R expression is mainly expressed in the hypothalamus and other brain regions [7], it is likely that the hepatic phenotype in MC4R-KO mice results from loss of function of MC4R in the brain, rather than in the liver itself. Accordingly, MC4R-KO mice would provide a novel rodent model with which to investigate the progression from diet-induced hepatic steatosis to NASH. Using this model, we have reported a unique histological structure in the liver termed hepatic crown-like structures (hCLS), in which macrophages surround dead or dying hepatocytes with large lipid droplets [8]. hCLS structurally resembles obesity-induced adipose tissue CLS [8], where sustained interaction between dead adipocytes and macrophages induces adipose tissue inflammation, thereby leading to systemic insulin resistance [9]. Interestingly, the number of hCLS is positively correlated with the extent of liver fibrosis, and myofibroblasts and collagen deposition are observed nearby hCLS [8], suggesting the role of hCLS in the development of NASH. We also detected hCLS in the liver of NAFLD/NASH patients [8]. On the basis of these observations, hCLS may be involved in disease progression from simple steatosis to NASH.

Fish oil rich in *n-3* polyunsaturated fatty acids (PUFAs) such as eicosapentaenoic acid (EPA) or *n-3* PUFAs are clinically effective to treat hypertriglyceridemia. As a molecular mechanism, *n-3* PUFAs improve hepatic lipid metabolism mainly by regulating transcription factors such as peroxisome proliferators-activated receptor α (PPARα) and sterol regulatory element binding protein-1c [10]. In addition, epidemiological and clinical trials have shown that *n-3* PUFAs significantly reduce the incidence of coronary heart disease [11], probably through their pleiotropic effect including an anti-inflammatory property. Given the suppressive effect on hepatic lipid accumulation and inflammation, *n-3* PUFAs could be therapeutically useful to prevent and/or treat NASH. Indeed, recent evidence suggests that *n-3* PUFAs effectively inhibit the development of the diet- or genetically-induced rodent models of NASH, whereas other studies failed [12–17]. However, the recent guideline pointed out that clinical efficacy of *n-3* PUFAs on NAFLD/NASH is controversial [18–25]. Moreover, it is still unclear which species in *n-3* PUFAs are responsible for the treatment of NASH and whether *n-3* PUFAs can regress the hepatic lesion after NASH develops.

In this study, we employed MC4R-KO mice to examine the effect of highly purified EPA on the development of NASH. EPA treatment markedly prevented hepatocyte injury, hCLS formation and collagen deposition along with lipid accumulation in the liver of MC4R-KO mice. Our data also showed that EPA treatment was effective after MC4R-KO mice developed NASH. Intriguingly, the improvement of liver fibrosis was in parallel with the reduction of

hCLS formation and hepatocyte injury, suggesting the involvement of hCLS in the beneficial effect of EPA. Collectively, this study raises a novel anti-fibrotic mechanism of EPA in a mouse model of NASH, thereby suggesting its therapeutic efficacy in NASH.

## Methods

### Materials

Preparation and characterization of highly purified EPA ethyl ester (purity: >98%, Mochida Pharmaceutical Co., Ltd., Tokyo, Japan) used in animal studies were reported elsewhere [26,27]. Ethyl palmitate (purity > 95%) was purchased from Wako (Tokyo, Japan).

### Animals

The MC4R-KO mice on the C57BL/6J background were a generous gift from Dr. Joel K. Elmquist (University of Texas Southwestern Medical Center) [6]. Male C57BL/6J wildtype mice were purchased from CLEA Japan (Tokyo, Japan). The animals were housed in individual cages in a temperature-, humidity- and light-controlled room (12-h light and 12-h dark cycle) and allowed free access to water and standard diet (SD) (CE-2; CLEA Japan). After 1-week acclimation period, 8 week-old male mice were given free access to water and either SD or Western diet (WD) (D12079B; Research Diets, New Brunswick, NJ) supplemented with 5% (wt/wt) ethyl palmitate or EPA ethyl ester [27]. Detailed dietary composition of the SD and WD is shown in S1 Table. All diets were changed every day and served with a non-metallic feeder to prevent oxidization of fatty acids. In this study, we conducted two experimental protocols to evaluate the preventive and therapeutic effect of EPA, *i.e.* EPA treatment throughout the experimental period (24 weeks) and 4-week EPA treatment after the development of NASH, respectively. At the end of the experiments, they were sacrificed, when fed *ad libitum*, under intraperitoneal pentobarbital anesthesia (30 mg/kg). All animal experiments were conducted in accordance to the guidelines for the care and use of laboratory animals of Tokyo Medical and Dental University. The protocol was approved by Tokyo Medical and Dental University Committee on Animal Research (No. 0140016A, No. 2011-207C3).

### Blood Analysis

Blood glucose levels were measured by the blood glucose test meter (Glutest PRO R; Sanwa-Kagaku, Nagoya Japan). Serum concentrations of alanine aminotransferase (ALT), triglyceride (TG), free fatty acid (FFA) and total cholesterol (TC) were measured by the respective standard enzymatic assays. Serum concentrations of adipocytokines were determined by the commercially available enzyme-linked immunosorbent assay (ELISA) kits (insulin: Morinaga, Tokyo, Japan; adiponectin: Otsuka Pharmaceutical, Tokyo, Japan; leptin: R&D systems, Minneapolis, MN). For insulin tolerance test, 1-hour fasted mice injected intraperitoneally with human insulin at 1.0 U/kg and blood glucose levels were determined before and at 15, 30, 60, 90 and 120 min after insulin administration.

### Hepatic TG Content

Total lipids in the liver were extracted with ice-cold 2:1 (vol/vol) chloroform/methanol. The TG concentrations were measured by an enzymatic assay kit (Wako Pure Chemicals, Osaka, Japan) [5].

## Quantification of Active TGFβ1 Content

Active transforming growth factor-β1 (TGFβ1) protein levels in the liver were measured as described [28]. Briefly, frozen liver samples were homogenizes in a lysis buffer (20 mM Tris, pH 7.5, 10 mM ethylenediaminetera-acetic acid) supplemented with protease inhibitors (2 mM phenylmethane sulfonyl fluoride, 0.5 mM dithiothreitol, protease inhibitor cocktail (Sigma, St. Louis, MO)). Samples were centrifuged at 17,000 x g for 20 min at 4°C and the supernatants were subjected to the ELISA kit for mouse TGFβ1 (R&D). Active TGFβ1 protein levels were normalized to the protein concentrations.

## Histological Analysis

The liver samples were fixed with neutral-buffered formalin and embedded in paraffin. Four-μm-thick sections were stained with Masson-trichrome and Sirius red [5]. The presence of F4/80-positive macrophages was detected immunohistochemically using the rat monoclonal anti-mouse F4/80 antibody described elsewhere [29]. Proteolytic activation of latent TGFβ was detected with antibody against R58 latency associated protein degradation products (LAP-DPs) [30]. Apoptotic cells were detected by TdT mediated dUTP-biotin nick end labeling (TUNEL) assay using ApopTag Plus Peroxidase In Situ Apoptosis Detection Kit (Millipore, Billerica, MA). The Sirius red-positive and R58 LAP-DP-positive areas were measured using the software WinROOF (Mitani, Chiba, Japan). TUNEL-positive cells were counted in the whole area of each section and expressed as the mean number/mm$^2$. The liver histology was assessed by two investigators without knowledge of the origin of the slides according to the NASH clinical research network scoring system [31].

## Quantitative Real-Time PCR

Total RNA was extracted from the liver using Sepasol reagent (Nacalai Tesque, Kyoto, Japan). Quantitative real-time PCR was performed with StepOnePlus Real-time PCR System using Fast SYBR Green Master Mix Reagent (Applied Biosystems, Foster City, CA) as described previously [5]. Primers used in this study were described in S2 Table. Levels of mRNA were normalized to those of 36B4 mRNA.

## Statistical Analysis

Data are presented as mean ± SE, and $P < 0.05$ was considered statistically significant. Statistical analysis was performed using analysis of variance followed by Scheffe's test. Differences between two groups were compared using Student *t*-test. Pearson correlation coefficient was employed to investigate the correlation among the numbers of hCLS and TUNEL-positive cells, and the extent of fibrosis.

# Results

## Preventive effect of EPA on hepatic lipid accumulation in MC4R-KO mice

First, we examined whether EPA treatment prevents the development of NASH using our mouse model of NASH. Wildtype mice were fed SD (WT-SD) and MC4R-KO mice were fed control diet, WD plus 5% weight palmitate (MC4R-control) or with the diet, in which 5% weight palmitate was replaced to EPA (MC4R-EPA Pre) for 24 weeks (Fig 1A). The amount of food intake was comparable between control and EPA-treated MC4R-KO mice (data not shown). The MC4R-KO mice fed control diet showed accelerated body weight gain relative to

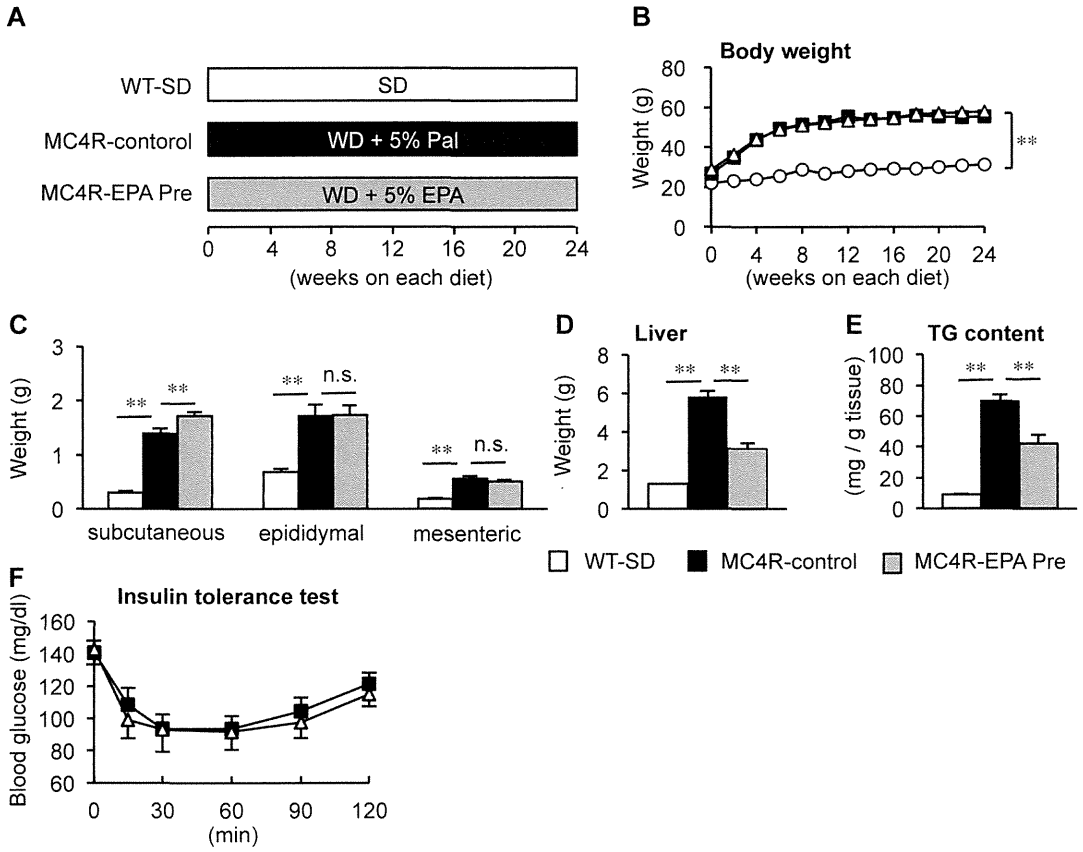


**Fig 1. Body weight and tissue weights in MC4R-KO mice treated with EPA for 24 weeks.** (A) Experimental protocol of preventive EPA treatment. Growth curve (B) and weights of the subcutaneous, epididymal and mesenteric white adipose tissues (C) and liver (D) of male MC4R-KO (MC4R) and wildtype (WT) mice. WT-SD, WT mice fed standard diet (SD); MC4R-control, MC4R-KO mice fed Western diet (WD) supplemented with 5% (wt/wt) palmitate; MC4R-EPA Pre, MC4R-KO mice fed WD supplemented with 5% (wt/wt) EPA for 24 weeks. Open circle, WT-SD; Open triangle, MC4R-control; closed square, MC4R-EPA Pre. (E) Liver triglyceride (TG) content at 24 weeks. (F) Insulin tolerance test (ITT) at 12-week WD feeding. Open triangle, MC4R-control; closed square, MC4R-EPA Pre. ** $P < 0.01$; n.s., not significant. WT-SD, $n = 8$; MC4R-control, $n = 7$; MC4R-EPA Pre, $n = 10$.

doi:10.1371/journal.pone.0121528.g001

wildtype mice fed SD, along with increased weights of adipose tissue and liver (Fig 1B–1D) as reported [5,8]. EPA treatment showed no appreciable or only marginal effect on body weight and adipose tissue weights (Fig 1B and 1C). On the other hand, the liver weight and the hepatic TG content were markedly reduced in EPA-treated MC4R-KO mice relative to control MC4R-KO mice ($P < 0.01$, Fig 1D and 1E). Hepatic fatty acid composition analysis revealed increased hepatic EPA content and decreased arachidonic acid content (S3 Table). EPA treatment also reduced serum concentrations of TC, FFA, and ALT in MC4R-KO mice, whereas EPA treatment did not affect glucose metabolism and insulin resistance (Table 1, Fig 1F). Since unbalanced production of pro- and anti-inflammatory adipocytokines in obesity has been implicated in the pathogenesis of NASH [32], we examined serum adipocytokine concentrations and found that EPA treatment significantly increased serum adiponectin concentrations in MC4R-KO mice (Table 1). On the other hand, EPA treatment did not affect serum concentrations of leptin in MC4R-KO mice (Table 1).

**Table 1. Serological parameters of MC4R-KO and WT mice treated with EPA for 24 weeks.**

| | WT | MC4R-KO | |
|---|---|---|---|
| | SD | Control | EPA-pre |
| BG (*ad lib*, mg/dL) | 144.0 ± 7.3 | 134.3 ± 9.7 | 119.1 ± 6.2 |
| Insulin (*ad lib*, ng/mL) | 0.6 ± 0.1 | 4.3 ± 1.3** | 3.7 ± 1.8 |
| TG (mg/dL) | 57.1 ± 30.9 | 30.9 ± 3.2** | 34.6 ± 6.0 |
| TC (mg/dL) | 70.8 ± 3.0 | 290.1 ± 15.0** | 122.5 ± 8.3¶ |
| FFA (mEq/L) | 1.13 ± 0.10 | 1.33 ± 0.09 | 0.80 ± 0.05¶ |
| ALT (IU/L) | 47.5 ± 5.6 | 539.1 ± 87.2** | 120.5 ± 16.8¶ |
| Adiponectin (μg/mL) | 12.7 ± 1.4 | 7.8 ± 1.0 | 17.7 ± 2.0¶ |
| Leptin (ng/mL) | 8.7 ± 1.8 | 114.3 ± 4.5** | 119.9 ± 8.9 |

WT, wildtype; SD, standard diet; BG, blood glucose; TG, triglyceride; FFA, free fatty acid; TC, total cholesterol; ALT, alanine aminotransferase. Data are expressed as the mean ± SE.

**$P < 0.01$ vs. WT-SD

¶ $P < 0.01$ vs. MC4R-Control. $n = 7–10$

doi:10.1371/journal.pone.0121528.t001

## Effect of EPA on the development of liver fibrosis in MC4R-KO mice

After 24 weeks, the livers from MC4R-KO mice fed control diet exhibited micro- and macrovesicular steatosis, ballooning degeneration, massive infiltration of inflammatory cells and pericellular fibrosis (Fig 2A and 2C) as reported previously [5,8]. On the other hand, steatotic changes and ballooning degeneration were markedly suppressed in EPA-treated MC4R-KO mice (Fig 2A and 2C). The fibrosis score and fibrosis area were also significantly decreased by EPA treatment (Fig 2B and 2D). Although the inflammation score was unchanged, the scores for steatosis and ballooning degeneration were decreased by EPA treatment, so that there was a significant reduction in NAS in EPA-treated MC4R-KO mice relative to control MC4R-KO mice (Fig 2E and 2F). In this study, mRNA expression of genes related to *de novo* lipogenesis (fatty acid synthase (FAS) and stearoyl-CoA desaturase-1 (SCD-1)) and β-oxidation (carnitine palmitoyltransferase 1A (CPT1A)) was markedly increased in the liver of control MC4R-KO mice relative to wildtype mice as reported [5], which was significantly suppressed by EPA treatment (Fig 3A and 3B). There was no apparent change in mRNA expression of proinflammatory genes such as (macrophage marker F4/80 and tumor necrosis factor-α (TNFα)) (Fig 3C). On the other hand, mRNA expression of TGFβ1-target genes such as collagen α1(I) (COL1A1), tissue inhibitor of metalloproteinase-1 (TIMP1) and matrix metalloproteinase-2 (MMP2) was significantly suppressed, although EPA treatment did not affect mRNA expression of TGFβ1 (Fig 3D). These observations, taken together, suggest that EPA treatment effectively prevents the development of liver fibrosis in MC4R-KO mice.

## Effect of EPA on hCLS formation and hepatocyte apoptosis in MC4R-KO mice

We have recently reported a unique histological structure or hCLS in the liver of MC4R-KO mice, where dead hepatocytes are surrounded by CD11c-positive macrophages [8]. Our data also suggest that hCLS promotes liver fibrosis during the progression from simple steatosis to NASH [8]. We found that EPA treatment effectively suppresses hCLS formation in MC4R-KO mice (Fig 4A), In this study, the F4/80-positive area was roughly comparable between the treatments (data not shown). Double immunofluorescent staining of F4/80 and CD11c revealed that hCLS-constituting macrophages are positive for CD11c in EPA-treated MC4R-KO mice

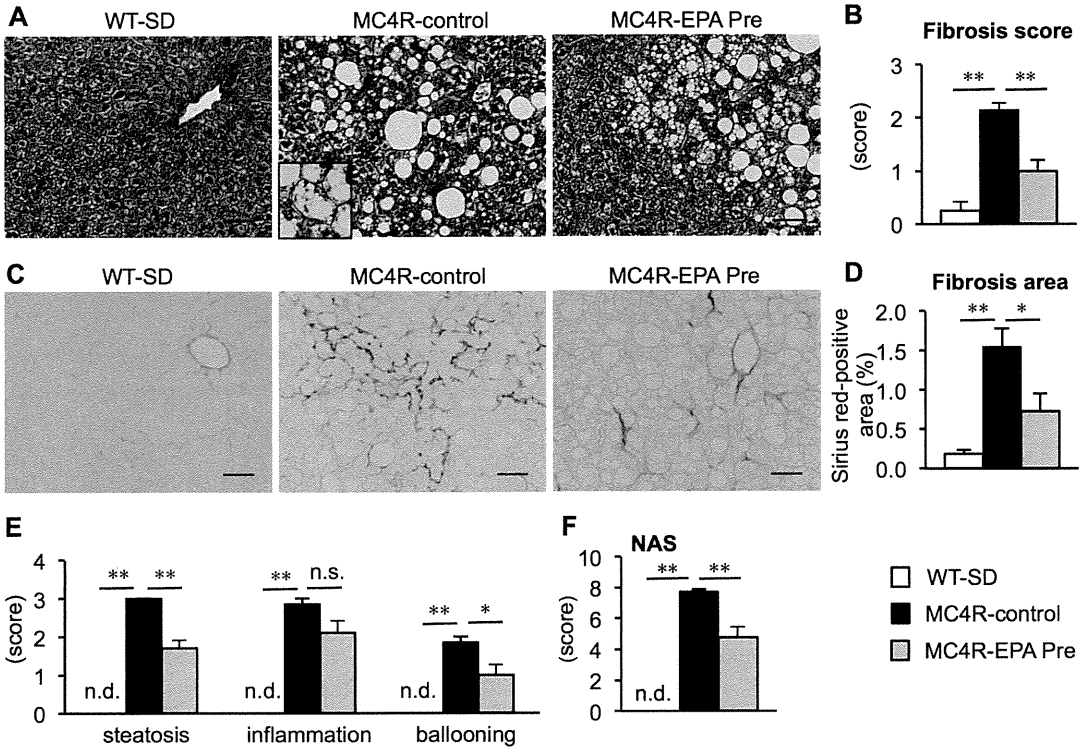


**Fig 2. Effect of EPA on liver injury and fibrosis in MC4R-KO mice.** Fibrillar collagen deposition evaluated by Masson-trichrome staining (A) and fibrosis scores (B) at 24 weeks. Inset: Representative image of hepatocyte ballooning. Sirius red staining (C) and quantification of Sirius red-positive area (D). Scores of steatosis, lobular inflammation, ballooning degeneration (E) and non-alcoholic fatty liver disease activity score (NAS) (F). Scale bars, 50 μm. * $P < 0.05$; ** $P < 0.01$; n.s., not significant; n.d., not detected. WT-SD, $n = 8$; MC4R-control, $n = 7$; MC4R-EPA Pre, $n = 10$.

doi:10.1371/journal.pone.0121528.g002

(Fig 4B), whereas hepatic mRNA expression of CD11c was significantly suppressed in EPA-treated MC4R-KO mice (Fig 4C) in parallel with reduced number of hCLS. Since hCLS-constituting macrophages are considered to engulf dead hepatocytes and residual lipids [33], we examined apoptotic cells by TUNEL staining. Compared to SD-fed wildtype mice, control MC4R-KO mice showed marked increase in the number of TUNEL-positive cells, most of which assembled around large lipid droplets (Fig 4D). TUNEL-positive cells were decreased in number in EPA-treated MC4R-KO mice relative to control MC4R-KO mice (Fig 4D), which was in parallel with serum ALT concentrations (Table 1). In this study, the number of hCLS was positively correlated with that of TUNEL-positive cells as well as the extent of liver fibrosis (Fig 4E and 4F) [8]. Collectively, these observations suggest that EPA suppresses hepatocyte apoptosis in MC4R-KO mice, which may prevent hCLS formation and fibrotic changes.

## Effect of EPA on hepatic TGFβ activation in MC4R-KO mice

Since there was no difference in hepatic TGFβ mRNA expression in MC4R-KO mice between the treatments, we next investigated the TGFβ activation state in the liver. We performed immunostaining using the anti-R58 LAP-DP antibody, which can detect the cleavage site of LAP, serving as a foot print for generation of active TGFβ [30]. The R58 LAP-DP-positive area was increased in the liver of control MC4R-KO mice relative to wildtype mice, which was decreased by EPA treatment (Fig 5A and 5B). The latent TGFβ is activated by plasma kallikrein

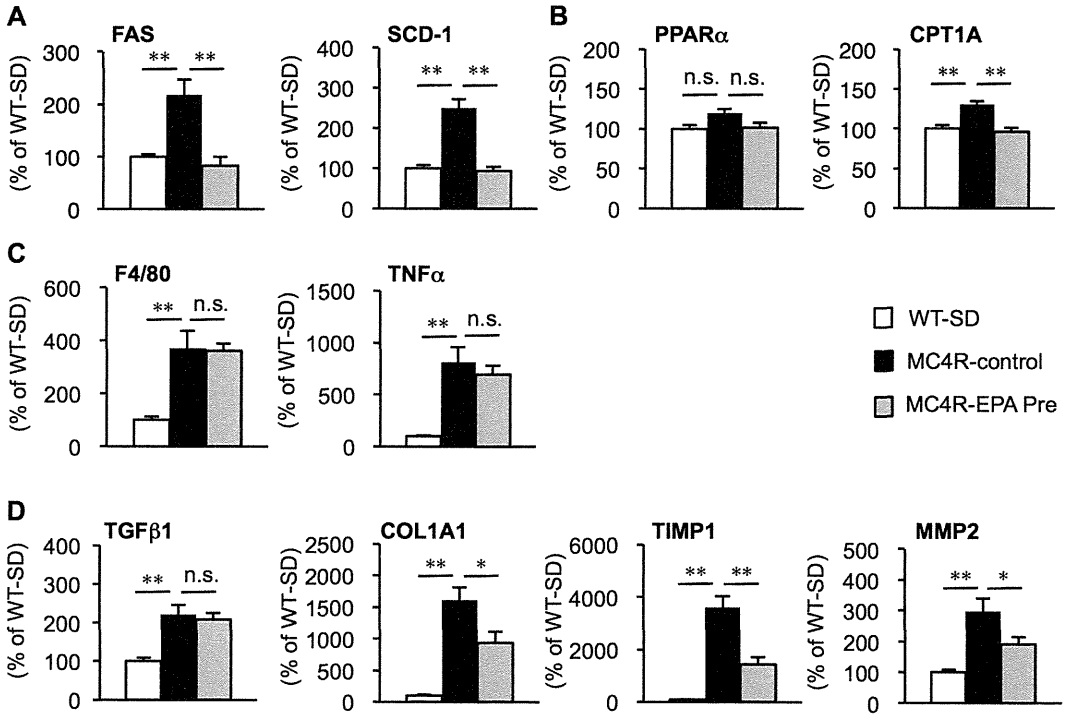


**Fig 3. Effect of EPA on hepatic mRNA expression in MC4R-KO mice.** Hepatic mRNA expression levels after 24 weeks of EPA treatment. mRNA expression of genes related to *de novo* lipogenesis (fatty acid synthase (FAS) and stearoyl-CoA desaturase (SCD-1)) (A), β-oxidation (peroxisome proliferators-activated receptor α PPARα and carnitine palmitoyltransferase 1A (CTP-1A)) (B), inflammatory markers (F4/80 and tumor necrosis factor α (TNFα) (C) and fibrogenic factors (transforming growth factor β1 (TGFβ1), collagen α1(I) (COL1A1), tissue inhibitor of metalloproteinase-1 (TIMP1) and matrix metalloproteinase-2 (MMP2)) (D). * $P < 0.05$; ** $P < 0.01$; n.s., not significant. WT-SD, $n = 8$; MC4R-control, $n = 7$; MC4R-EPA Pre, $n = 10$.

doi:10.1371/journal.pone.0121528.g003

that is bound to urokinase-type plasminogen activator receptor (uPAR) on the cell surface [34]. In this study, mRNA expression of uPAR was significantly decreased in EPA-treated MC4R-KO mice (Fig 5C). We also confirmed the decreased protein levels of active TGFβ in the liver of EPA-treated MC4R-KO mice (Fig 5D). These observations suggest that EPA suppresses TGFβ activation, thereby inhibiting disease progression from simple steatosis to NASH.

## Therapeutic effect of EPA on the progression of NASH in MC4R-KO mice

We also examined whether EPA treatment is effective after 20 weeks of control diet feeding when MC4R-KO mice develop NASH [8]. In this study, MC4R-KO mice were fed either control diet (MC4R-KO control) or EPA-supplemented diet (MC4R-EPA Tx) for another 4 weeks (Fig 6A). The liver weight and hepatic TG content were significantly reduced in EPA-treated MC4R-KO mice relative to control MC4R-KO mice at 24 weeks, whereas body weight and adipose tissue weight except for the epididymal fat depot were unchanged between the groups (S1A–S1D Fig.). Serum concentrations of TC and ALT were reduced, and those of adiponectin were increased in EPA-treated MC4R-KO mice (S4 Table). In this study, histological analysis revealed that EPA treatment for 4 weeks significantly suppressed the progression of liver fibrosis in MC4R-KO mice (Fig 6B–6D). Moreover, the NAS was significantly decreased in EPA-treated MC4R-KO mice relative to control MC4R-KO mice, although the change in each NAS

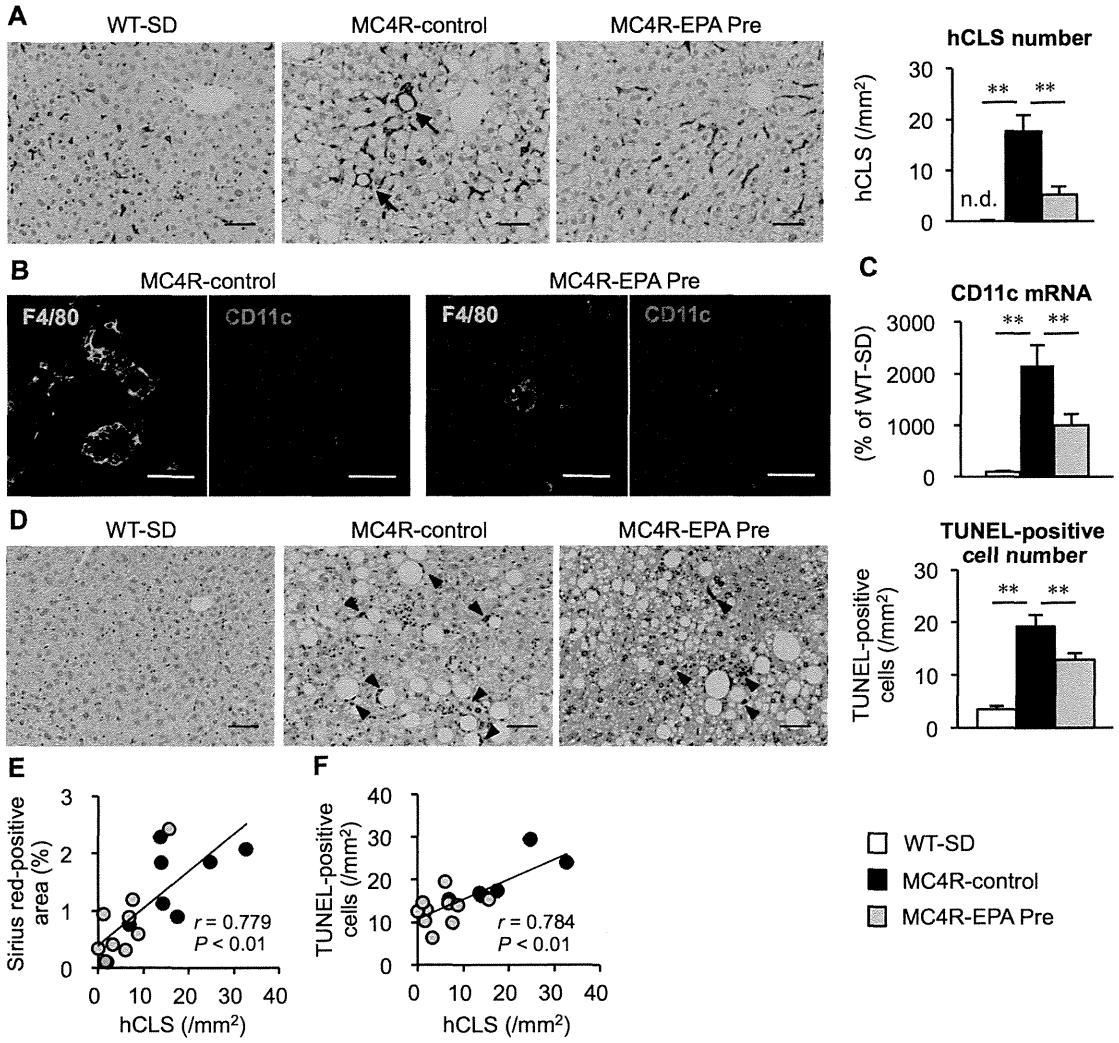


**Fig 4. Effect of EPA on hCLS formation and apoptosis in the liver of MC4R-KO mice.** (A) F4/80 immunostaining of the liver after 24 weeks of EPA treatment. Arrows indicate characteristic histological features termed "hepatic crown-like structures (hCLS)". (B) Immunofluorescent staining for F4/80 (green) and CD11c (red). (C) Hepatic mRNA expression of CD11c. (D) TdT mediated dUTP-biotin nick end labeling (TUNEL) immunostaining and the number of TUNEL-positive cells. Arrowheads indicate TUNEL-positive cells. Correlation of the number of hCLS and the fibrosis area (E) and the number of TUNEL-positive cells (F). Scale bars, 50 μm. * $P < 0.05$; ** $P < 0.01$; n.d., not detected. WT-SD, $n = 8$; MC4R-control, $n = 7$; MC4R-EPA Pre, $n = 10$.

doi:10.1371/journal.pone.0121528.g004

component (steatosis, inflammation, and ballooning degeneration) did not reach statistic significance (Fig 6E and 6F). Similar to the preventive protocol, hepatic mRNA expression of genes related to *de novo* lipogenesis, β-oxidation, and fibrogenesis was decreased in EPA-treated MC4R-KO mice relative to control MC4R-KO mice (S2 Fig.). The number of hCLS was also significantly reduced in EPA-treated MC4R-KO mice relative to control MC4R-KO mice, along with down-regulation of CD11c mRNA expression (S3A–S3D Fig.). Furthermore, EPA treatment resulted in a significant reduction in the number of TUNEL-positive cells and TGFβ activation (S3E–S3H Fig.). These observations, taken together, suggest that EPA suppressed the progression of liver fibrosis in MC4R-KO mice after the mice developed NASH.

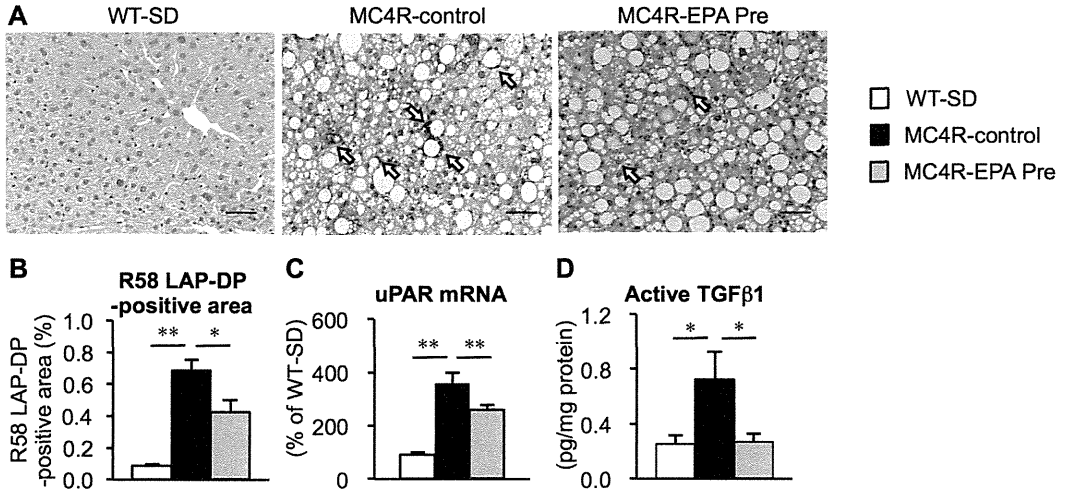


**Fig 5. Effect of EPA on hepatic TGFβ activation in MC4R-KO mice.** (A) Immmunostaining with anti-R58 LAP-DP antibody to determine TGFβ activation in the liver after 24 weeks of EPA treatment. (B) Quantification of the R58 LAP-DP-positive area. (C) Hepatic mRNA expression of urokinase-type plasminogen activator receptor (uPAR). (D) Active TGFβ protein levels in the liver. Scale bars, 50 μm. * $P < 0.05$; ** $P < 0.01$. WT-SD, $n = 8$; MC4R-control, $n = 7$; MC4R-EPA Pre, $n = 10$.

doi:10.1371/journal.pone.0121528.g005

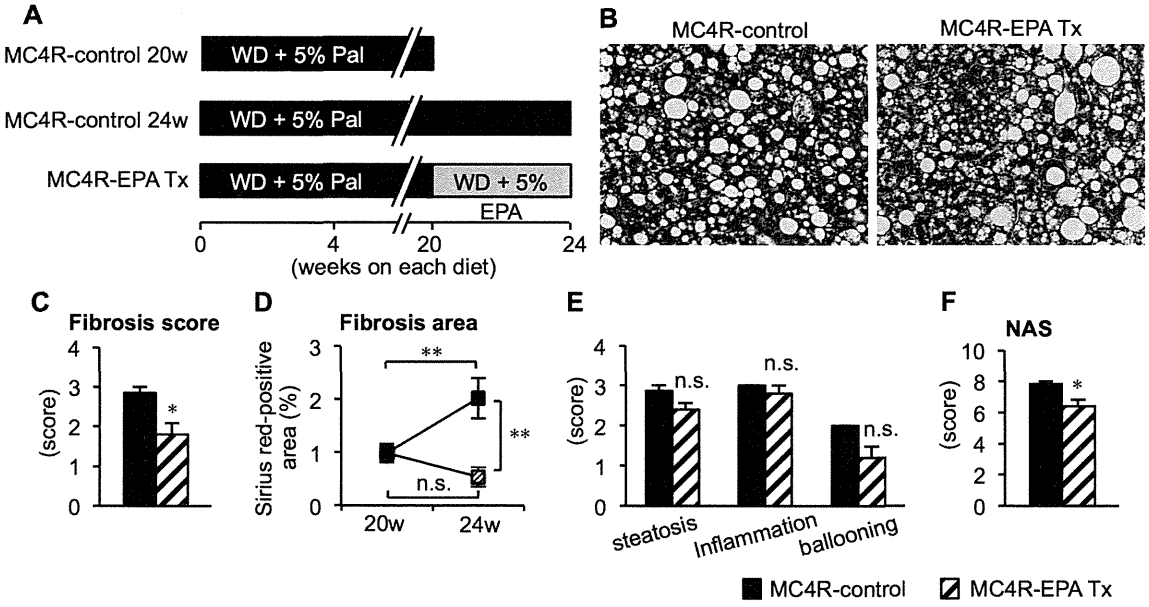


**Fig 6. Histological analysis of the liver of MC4R-KO mice treated with EPA for 4 weeks after the development of NASH.** (A) Experimental protocol of therapeutic EPA treatment. Fibrillar collagen deposition evaluated by Masson-trichrome staining (B) and fibrosis scores (C). (D) Quantification of Sirius red-positive area. Scores of steatosis, lobular inflammation, ballooning degeneration (E) and NAS (F). Scale bars, 50 μm. * $P < 0.05$; ** $P < 0.01$; n.s., not significant. MC4R-control, $n = 7$; MC4R-EPA Pre, $n = 10$.

doi:10.1371/journal.pone.0121528.g006

## Discussion

Using a variety of animal models through genetic, dietary, and/or pharmacologic approaches, many attempts have been made to identify novel therapeutic strategies for NASH, while their clinical efficacy is still unclear. It is partly because of the limited availability of appropriate animal models that reflect a liver condition of human NASH [35]. For instance, dietary deficiency of methionine and choline develops steatosis and mild fibrosis in the liver, although without obesity and insulin resistance [35]. Since NASH is considered as the hepatic phenotype of the metabolic syndrome, crosstalk among multiple organs should be involved in the pathophysiology of NASH. In this regard, MC4R-KO mice, a unique rodent model of NASH accompanied by obesity and systemic insulin resistance, would be useful for evaluating the effectiveness of novel drugs to treat NASH. This is the first report to evaluate drug efficacy using MC4R-KO mice. In this study, we demonstrate that EPA treatment effectively suppresses the development and progression of liver fibrosis along with marked reduction of hepatic steatosis, without affecting body weight. These observations suggest a clinical implication of EPA for the treatment of NASH.

We previously reported that hCLS plays an important role in the progression from simple steatosis to NASH [8]. Since EPA treatment markedly suppressed hCLS formation as well as interstitial fibrosis in MC4R-KO mice, it is likely that one site of actions of EPA is hCLS. Given that CD11c-positive macrophages surround dead hepatocytes in hCLS, EPA may suppress hepatocyte injury and cell death. This notion is supported by our observations that EPA treatment effectively prevented the increase in the number of TUNEL-positive cells, serum ALT concentrations, and the hepatocyte injury score (ballooning) in MC4R-KO mice. Moreover, these effects were observed even when MC4R-KO mice were treated with EPA after NASH developed. During the development of NASH, hepatocytes store excessive lipid including toxic lipids (*i.e.* saturated free fatty acid, free cholesterol, and lysophosphatidyl choline), which leads to metabolic stress such as oxidative stress and endoplasmic reticulum stress, thereby activating the cell death program [1,36,37]. Notably, hepatocyte apoptosis is a prominent feature of human NASH as well [38]. In this regard, it is known that that *n-3* PUFAs can induce gene expression of ROS-degrading enzymes to inhibit oxidative stress, and antagonize the saturated fatty acid-induced endoplasmic reticulum stress [39,40]. It is, therefore, conceivable that EPA treatment ameliorates lipotoxicity of hepatocytes to prevent the formation of hCLS in MC4R-KO mice.

Fibrogenesis is a complex process that involves a variety of cells including both parenchymal cells and stromal cells like myofibroblasts and immune cells. Although EPA and *n-3* PUFAs are known to exert an anti-inflammatory property [10,41], EPA treatment did not affect the inflammation score and TNFα mRNA expression in the liver from MC4R-KO mice. TGFβ, a key regulator of fibrogenesis, is produced as a latent complex containing latency-associated protein and latent TGFβ binding protein, and then activated when released from the latent complex [30]. In this study, expression of uPAR, a cell surface receptor for plasma kallikrein, was increased in the liver of MC4R-KO mice, suggesting the plasma kallikrein-mediated TGFβ activation. Intriguingly, uPAR expression and active TGFβ levels were markedly suppressed by EPA treatment. Among several molecules that can activate TGFβ such as integrins, metalloproteinases and plasmin, plasma kallikrein plays an important role in animal models of liver fibrosis [34,42]. Since TNFα potently induces uPAR expression in cultured hepatic stellate cells [34], it is interesting to know how hCLS formation induces TGFβ activation during the development of NASH and how EPA suppresses the process.

We previously reported that complex interactions between adipose tissue and liver should play a role in the development of NASH in MC4R-KO mice [5]. For instance, unbalanced

production of pro- and anti-inflammatory adipocytokines in obesity has been implicated in the pathogenesis of obesity-related complications including NASH [43]. Among numerous adipocytokines, there is substantial evidence on the protective role of adiponectin in the development of hepatic fibrosis and inflammation [44,45]. As a possible mechanism, adiponectin stimulates β-oxidation by activation of AMP-activated protein kinase and PPARα and down regulates expression of sterol regulatory element binding protein-1c to suppress *de novo* lipogenesis in the liver [46,47]. Adiponectin also exerts its inhibitory effect on platelet-derived growth factor BB- and TGFβ-induced proliferation and migration of hepatic stellate cells [48]. In this study, EPA treatment effectively increased the otherwise reduced serum adiponectin concentrations in MC4R-KO mice, which may be involved in the beneficial effect of EPA on liver injury. As we and others reported previously, serum adiponectin concentrations are elevated in obese mice and humans when treated with EPA or *n-3* PUFA-rich fish oil [26,49,50]. Moreover, we have provided evidence that EPA increases adiponectin secretion through the improvement of obesity-induced adipose tissue inflammation [26]. Neschen *et al.* also showed that fish oil activates PPARγ in adipocytes to increase adiponectin secretion [49]. On the other hand, EPA treatment did not show the effect on the serum concentrations of leptin in MC4R-KO mice, while it is known that leptin promotes liver fibrosis in certain liver fibrosis models [28,51,52]. Collectively, adipose tissue may contribute to the pathogenesis of liver fibrosis in MC4R-KO mice. It is, therefore, conceivable that the beneficial effect of EPA on liver injury of MC4R-KO mice is attributed to its action on adipose tissue as well as liver.

Clinical efficacy of *n-3* PUFAs for the treatment of NAFLD/NASH is still controversial. Tanaka *et al.* reported that highly purified EPA treatment improves biochemical and histological abnormalities in Japanese patients with NASH [21]. In contrast, a recent randomized, double-blind, placebo-controlled trial failed to prove the effectiveness of EPA for 12 months on hepatic steatosis and liver fibrosis in patients with NAFLD/NASH [22,23]. It is noteworthy that the dosage of EPA used in this study might not be enough for American population, where the well-established beneficial effect of EPA on dyslipidemia was not observed [22,23]. There was also no significant improvement in liver histology in several clinical trials using *n-3* PUFAs, in which the treatment showed only marginal effect on dyslipidemia [23–25]. Therefore, additional studies are required regarding the dosage of EPA and duration of the treatment. Moreover, dietary saturated fatty acid composition may affect the efficacy of EPA treatment, since experimental evidence in rodents suggest that EPA exerts its anti-inflammatory property, at least in part, through counteracting saturated fatty acids [26], and diet rich in saturated fatty acids augments insulin resistance and NAFLD [53,54]. Based on the heterogeneity of NAFLD/NASH patients, it is also important to evaluate the effect of EPA in subgroups with differential risk factors.

In conclusion, we demonstrate that EPA treatment effectively prevents the development and progression of liver fibrosis in MC4R-KO mice along with marked reduction of hepatic steatosis. EPA may exert its anti-fibrotic effect through suppression of hepatocyte injury-induced TGFβ activation in hCLS. Our data also suggest that EPA acts on adipose tissue as well as liver to ameliorate liver fibrosis. This study unravels a novel anti-fibrotic mechanism of EPA, thereby suggesting a clinical implication for the treatment of NASH.

## Supporting Information

**S1 Fig. Body weight and tissue weights in MC4R-KO mice in the therapeutic study.** Body weight (A) and weights of the subcutaneous, epididymal, and mesenteric white adipose tissues (B) and liver (C) of male MC4R-KO before EPA treatment (Western diet (WD) supplemented with 5% (wt/wt) palmitate for 20 weeks) and after 4-week EPA treatment. MC4R-EPA Tx,

MC4R-KO mice fed WD supplemented with 5% (wt/wt) EPA for 4 weeks after the development of NASH. (D) Liver triglyceride (TG) content at each time point. †† $P < 0.01$ vs. MC4R-control at 20 weeks; ** $P < 0.01$ vs. MC4R-control at 24 weeks; n.s., not significant. MC4R-control at 20 weeks, $n = 9$; MC4R-control at 24 weeks, $n = 7$; MC4R-EPA Tx, $n = 10$.
(TIF)

**S2 Fig. Hepatic mRNA expression in MC4R-KO mice in the therapeutic study.** Hepatic mRNA expression levels after 4-week EPA treatment. mRNA expression of *de novo* lipogenesis (FAS and SCD-1) (fatty acid synthase (FAS) and stearoyl-CoA desaturase (SCD-1)) and β-oxidation (PPARα, CPT1A) (A), inflammatory markers (F4/80 and tumor necrosis factor α (TNFα) (B) and fibrogenic factors (transforming growth factor β1 (TGFβ1), collagen α1(I) (COL1A1), tissue inhibitor of metalloproteinase-1 (TIMP1), and matrix metalloproteinase-2 (MMP2)) (C). * $P < 0.05$; ** $P < 0.01$; n.s., not significant.
(TIF)

**S3 Fig. hCLS formation and TGFβ activation in the liver of MC4R-KO mice in the therapeutic study.** (A) F4/80 immunostaining. Arrows indicate hepatic crown-like structures (hCLS). (B) Quantification of hCLS number after EPA treatment. (C) Immunofluorescent analysis for F4/80 and CD11c. (D) Hepatic mRNA expression of CD11c. Quantification of the TUNEL-positive cell number (E) and R58 LAP-DP-positive area (F). (G) Hepatic mRNA expression of urokinase-type plasminogen activator receptor (uPAR). (H) Active TGFβ1 protein levels in the liver. Scale bars, 50 μm. * $P < 0.05$; ** $P < 0.01$.
(TIF)

**S1 Table. Dietary composition of standard diet (CE-2) and Western diet (D12079B) used in this study.**
(DOCX)

**S2 Table. Primers used in this study.**
(DOCX)

**S3 Table. Fatty acid composition of the liver from MC4R-KO treated with EPA for 24 weeks.**
(DOCX)

**S4 Table. Serological parameters of MC4R-KO mice in the therapeutic study.**
(DOCX)

## Acknowledgments

We thank Dr. Joel K. Elmquist (University of Texas Southwestern Medical Center) for the generous gift of MC4R-KO mice. We also thank Ms. Yumi Gotoda for secretarial and technical assistances and the members of the Ogawa laboratory for helpful discussions.

## Author Contributions

Conceived and designed the experiments: MI T. Suganami. Performed the experiments: KK MI S. Kanai NN T. Sakai. Analyzed the data: KK MI. Contributed reagents/materials/analysis tools: HK MH S. Kojima. Wrote the paper: MI T. Suganami YO. Provided expertise and contributed discussion: YI.

## References


1. Farrell GC, Larter CZ. Nonalcoholic fatty liver disease: from steatosis to cirrhosis. Hepatology 2006; 43: S99–S112. PMID: 16447287
2. Day CP, James OF. Steatohepatitis: a tale of two "hits"? Gastroenterology 1998; 114: 842–845. PMID: 9547102
3. Browning JD, Horton JD. Molecular mediators of hepatic steatosis and liver injury. J Clin Invest 2004; 114: 147–152. PMID: 15254578
4. Neuschwander-Tetri BA. Hepatic lipotoxicity and the pathogenesis of nonalcoholic steatohepatitis: the central role of nontriglyceride fatty acid metabolites. Hepatology 2010; 52: 774–788. doi: 10.1002/hep.23719 PMID: 20683968
5. Itoh M, Suganami T, Nakagawa N, Tanaka M, Yamamoto Y, Kamei Y, et al. Melanocortin 4 receptor-deficient mice as a novel mouse model of nonalcoholic steatohepatitis. Am J Pathol 2011; 179: 2454–2463. doi: 10.1016/j.ajpath.2011.07.014 PMID: 21906580
6. Balthasar N, Dalgaard LT, Lee CE, Yu J, Funahashi H, Williams T, et al. Divergence of melanocortin pathways in the control of food intake and energy expenditure. Cell 2005; 123: 493–505. PMID: 16269339
7. Gautron L, Lee C, Funahashi H, Friedman J, Lee S, Elmquist JK. Melanocortin-4 receptor expression in a vago-vagal circuitry involved in postprandial functions. J Comp Neurol 2010; 518: 6–24. doi: 10.1002/cne.22221 PMID: 19882715
8. Itoh M, Kato H, Suganami T, Konuma K, Marumoto Y, Terai S, et al. Hepatic crown-like structure: a unique histological feature in non-alcoholic steatohepatitis in mice and humans. PloS one 2013; 8: e82163. doi: 10.1371/journal.pone.0082163 PMID: 24349208
9. Hotamisligil GS. Inflammation and metabolic disorders. Nature 2006; 444: 860–867. PMID: 17167474
10. Jump DB. The biochemistry of *n-3* polyunsaturated fatty acids. J Biol Chem 2002; 277: 8755–8758. PMID: 11748246
11. Kris-Etherton PM, Harris WS, Appel LJ. Fish consumption, fish oil, omega-3 fatty acids, and cardiovascular disease. Circulation 2002; 106: 2747–2757. PMID: 12438303
12. Larter CZ, Yeh MM, Cheng J, Williams J, Brown S, dela Pena A, et al. Activation of peroxisome proliferator-activated receptor α by dietary fish oil attenuates steatosis, but does not prevent experimental steatohepatitis because of hepatic lipoperoxide accumulation. J Gastroenterol Hepatol 2008; 23: 267–275. PMID: 17868330
13. Ishii H, Horie Y, Ohshima S, Anezaki Y, Kinoshita N, Dohmen T, et al. Eicosapentaenoic acid ameliorates steatohepatitis and hepatocellular carcinoma in hepatocyte-specific Pten-deficient mice. J Hepatol 2009; 50: 562–571. doi: 10.1016/j.jhep.2008.10.031 PMID: 19162361
14. Kajikawa S, Harada T, Kawashima A, Imada K, Mizuguchi K. Highly purified eicosapentaenoic acid ethyl ester prevents development of steatosis and hepatic fibrosis in rats. Dig Dis Sci 2010; 55: 631–641. doi: 10.1007/s10620-009-1020-0 PMID: 19856102
15. Kajikawa S, Imada K, Takeuchi T, Shimizu Y, Kawashima A, Harada T, et al. Eicosapentaenoic acid attenuates progression of hepatic fibrosis with inhibition of reactive oxygen species production in rats fed methionine- and choline-deficient diet. Dig Dis Sci 2011; 56: 1065–1074. doi: 10.1007/s10620-010-1400-5 PMID: 20848203
16. Depner CM, Philbrick KA, Jump DB. Docosahexaenoic acid attenuates hepatic inflammation, oxidative stress, and fibrosis without decreasing hepatosteatosis in a *Ldlr(-/-)* mouse model of western diet-induced nonalcoholic steatohepatitis. J Nutr 2013; 143: 315–323. doi: 10.3945/jn.112.171322 PMID: 23303872
17. Svegliati-Baroni G, Candelaresi C, Saccomanno S, Ferretti G, Bachetti T, Marzione M, et al. A model of insulin resistance and nonalcoholic steatohepatitis in rats: role of peroxisome proliferator-activated receptor-α and n-3 polyunsaturated fatty acid treatment on liver injury. Am J Pathol 2006; 169: 846–860. PMID: 16936261
18. Chalasani N, Younossi Z, Lavine JE, Diehl AM, Brunt EM, Cusi K, et al. The diagnosis and management of non-alcoholic fatty liver disease: practice guideline by the American Gastroenterological Association, American Association for the Study of Liver Diseases, and American College of Gastroenterology. Gastroenterology 2012; 142: 1592–1609. doi: 10.1053/j.gastro.2012.04.001 PMID: 22656328
19. Capanni M, Calella F, Biagini MR, Genise S, Raimondi L, Bedogni G, et al. Prolonged *n-3* polyunsaturated fatty acid supplementation ameliorates hepatic steatosis in patients with non-alcoholic fatty liver disease: a pilot study. Aliment Pharmacol Ther 2006; 23: 1143–1151. PMID: 16611275

20. Di Minno MN, Russolillo A, Lupoli R, Ambrosino P, Di Minno A, Tarantino G. Omega-3 fatty acids for the treatment of non-alcoholic fatty liver disease. World J Gastroenterol 2012; 18: 5839–5847. doi: 10.3748/wjg.v18.i41.5839 PMID: 23139599

21. Tanaka N, Sano K, Horiuchi A, Tanaka E, Kiyosawa K, Aoyama T. Highly purified eicosapentaenoic acid treatment improves nonalcoholic steatohepatitis. J Clin Gastroenterol 2008; 42: 413–418. doi: 10.1097/MCG.0b013e31815591aa PMID: 18277895

22. Sanyal AJ, Abdelmalek MF, Suzuki A, Cummings OW, Chojkier M; EPA-A Study Group. No significant effects of ethyl-eicosapentanoic acid on histologic features of nonalcoholic steatohepatitis in a phase 2 trial. Gastroenterology 2014; 147: 377–384 e371. doi: 10.1053/j.gastro.2014.04.046 PMID: 24818764

23. Scorletti E, Bhatia L, McCormick KG, Clough GF, Nash K, Hadson L, et al. Effects of purified eicosapentaenoic and docosahexaenoic acids in non-alcoholic fatty liver disease: Results from the *WELCOME study. Hepatology 2014 Jul 4. doi: 10.1002/hep.27289

24. Dasarathy S, Dasarathy J, Khiyami A, Yerian L, Hawkins C, Sargent R, et al. Double-blind randomized placebo-controlled clinical trial of omega 3 fatty acids for the treatment of diabetic patients with nonalcoholic steatohepatitis. J Clin Gastroenterol 2015; 49: 137–144. doi: 10.1097/MCG.0000000000000099 PMID: 24583757

25. Argo CK, Patrie JT, Lackner C, Henry TD, deLange EE, Weltman AL, et al. Effects of n-3 fish oil on metabolic and histological parameters in NASH: A double-blind, randomized, placebo-controlled trial. J Hepatol 2015; 62: 190–197. doi: 10.1016/j.jhep.2014.08.036 PMID: 25195547

26. Itoh M, Suganami T, Satoh N, Tanimoto-Koyama K, Yuan X, Tanaka M, et al. Increased adiponectin secretion by highly purified eicosapentaenoic acid in rodent models of obesity and human obese subjects. Arterioscler Thromb Vasc Biol 2007; 27: 1918–1925. PMID: 17569885

27. Sato A, Kawano H, Notsu T, Ohta M, Nakakuki M, Mizuguchi K, et al. Antiobesity effect of eicosapentaenoic acid in high-fat/high-sucrose diet-induced obesity: importance of hepatic lipogenesis. Diabetes 2010; 59: 2495–2504. doi: 10.2337/db09-1554 PMID: 20682690

28. Leclercq IA, Farrell GC, Schriemer R, Robertson GR. Leptin is essential for the hepatic fibrogenic response to chronic liver injury. J Hepatol 2002; 37: 206–213. PMID: 12127425

29. Kitagawa K, Wada T, Furuichi K, Hashimoto H, Ishiwata Y, Asano M, et al. Blockade of CCR2 ameliorates progressive fibrosis in kidney. Am J Pathol 2004; 165: 237–246. PMID: 15215179

30. Hara M, Kirita A, Kondo W, Matsuura T, Nagatsuma K, Dohmae N, et al. LAP degradation product reflects plasma kallikrein-dependent TGF-β activation in patients with hepatic fibrosis. SpringerPlus 2014; 3: 221. doi: 10.1186/2193-1801-3-221 PMID: 24877031

31. Juluri R, Vuppalanchi R, Olson J, Unalp A, Van Natta ML, Cummings OW, et al. Generalizability of the Nonalcoholic Steatohepatitis Clinical Research Network Histologic Scoring System for Nonalcoholic Fatty Liver Disease. J Clin Gastroenterol 2010; 45: 55–58.

32. Marra F, Bertolani C. Adipokines in liver diseases. Hepatology 2009; 50: 957–969. doi: 10.1002/hep.23046 PMID: 19585655

33. Ioannou GN, Haigh WG, Thorning D, Savard C. Hepatic cholesterol crystals and crown-like structures distinguish NASH from simple steatosis. J Lipid Res 2013; 54: 1326–1334. doi: 10.1194/jlr.M034876 PMID: 23417738

34. Akita K, Okuno M, Enya M, Imai S, Moriwaki H, Kawada N, et al. Impaired liver regeneration in mice by lipopolysaccharide via TNF-α/kallikrein-mediated activation of latent TGF-β. Gastroenterology 2002; 123: 352–364. PMID: 12105863

35. Varela-Rey M, Embade N, Ariz U, Lu SC, Mato JM, Martinez-Chantar ML. Non-alcoholic steatohepatitis and animal models: understanding the human disease. Int J Biochem Cell Biol 2009; 41: 969–976. doi: 10.1016/j.biocel.2008.10.027 PMID: 19027869

36. Larter CZ, Yeh MM, Haigh WG, Williams J, Brown S, Bell-Anderson KS, et al. Hepatic free fatty acids accumulate in experimental steatohepatitis: role of adaptive pathways. J Hepatol 2008; 48: 638–647. doi: 10.1016/j.jhep.2007.12.011 PMID: 18280001

37. Kakisaka K, Cazanave SC, Fingas CD, Guicciardi ME, Bronk SF, Werneburg NW, et al. (2012) Mechanisms of lysophosphatidylcholine-induced hepatocyte lipoapoptosis. Am J Physiol Gastrointest Liver Physiol 2012; 302: G77–84. doi: 10.1152/ajpgi.00301.2011 PMID: 21995961

38. Feldstein AE, Canbay A, Angulo P, Taniai M, Burgart LJ, Lindor KD, et al. Hepatocyte apoptosis and fas expression are prominent features of human nonalcoholic steatohepatitis. Gastroenterology 2003; 125: 437–443. PMID: 12891546

39. Richard D, Kefi K, Barbe U, Bausero P, Visioli F. Polyunsaturated fatty acids as antioxidants. Pharmacol Res 2008; 57: 451–455. doi: 10.1016/j.phrs.2008.05.002 PMID: 18583147

40. Cazanave SC, Gores GJ. Mechanisms and clinical implications of hepatocyte lipoapoptosis. Clin Lipidol 2010; 5: 71–85. PMID: 20543905

41. Calder PC. Omega-3 polyunsaturated fatty acids and inflammatory processes: nutrition or pharmacology? Br J Clin Pharmacol 2013; 75: 645–662. doi: 10.1111/j.1365-2125.2012.04374.x PMID: 22765297

42. Okuno M, Akita K, Moriwaki H, Kawada N, Ikeda K, Kaneda K, et al. Prevention of rat hepatic fibrosis by the protease inhibitor, camostat mesilate, via reduced generation of active TGF-β. Gastroenterology 2001; 120: 1784–1800. PMID: 11375959

43. Day CP. From fat to inflammation. Gastroenterology 2006; 130: 207–210. PMID: 16401483

44. Kamada Y, Matsumoto H, Tamura S, Fukushima J, Kiso S, Fukui K, et al. Hypoadiponectinemia accelerates hepatic tumor formation in a nonalcoholic steatohepatitis mouse model. J Hepatol 2007; 47: 556–564. PMID: 17459514

45. Asano T, Watanabe K, Kubota N, Gunji T, Omata M, Kadowaki T, et al. Adiponectin knockout mice on high fat diet develop fibrosing steatohepatitis. J Gastroenterol Hepatol 2009; 24: 1669–1676. doi: 10.1111/j.1440-1746.2009.06039.x PMID: 19788607

46. Xu A, Wang Y, Keshaw H, Xu LY, Lam KS, Cooper GJ. The fat-derived hormone adiponectin alleviates alcoholic and nonalcoholic fatty liver diseases in mice. J Clin Invest 2003; 112: 91–100. PMID: 12840063

47. Shklyaev S, Aslanidi G, Tennant M, Prima V, Kohlbrenner E, Kroutov V, et al. Sustained peripheral expression of transgene adiponectin offsets the development of diet-induced obesity in rats. Proc Natl Acad Sci U S A 2003; 100: 14217–14222. PMID: 14617771

48. Kamada Y, Tamura S, Kiso S, Matsumoto H, Saji Y, Yoshida Y, et al. Enhanced carbon tetrachloride-induced liver fibrosis in mice lacking adiponectin. Gastroenterology 2003; 125: 1796–1807. PMID: 14724832

49. Neschen S, Morino K, Rossbacher JC, Pongratz RL, Cline GW, Sono S, et al. Fish oil regulates adiponectin secretion by a peroxisome proliferator-activated receptor-γ-dependent mechanism in mice. Diabetes 2006; 55: 924–928. PMID: 16567512

50. Flachs P, Mohamed-Ali V, Horakova O, Rossmeisl M, Hosseinzadeh-Attar MJ, Hensler M, et al. Polyunsaturated fatty acids of marine origin induce adiponectin in mice fed a high-fat diet. Diabetologia 2006; 49: 394–397. PMID: 16397791

51. Aleffi S, Petrai I, Bertolani C, Parola M, Colombatto S, Novo E, et al. Upregulation of proinflammatory and proangiogenic cytokines by leptin in human hepatic stellate cells. Hepatology 2005; 42: 1339–1348. PMID: 16317688

52. Saxena NK, Ikeda K, Rockey DC, Friedman SL, Anania FA. Leptin in hepatic fibrosis: evidence for increased collagen production in stellate cells and lean littermates of *ob/ob* mice. Hepatology 2002; 35: 762–771. PMID: 11915021

53. Wang D, Wei Y, Pagliassotti MJ. Saturated fatty acids promote endoplasmic reticulum stress and liver injury in rats with hepatic steatosis. Endocrinology 2006; 157: 943–951.

54. Savard C, Tartaglione EV, Kuver R, Haigh WG, Farrell GC, Subramanian S, et al. Synergistic interaction of dietary cholesterol and dietary fat in inducing experimental steatohepatitis. Hepatology 2013; 57: 81–92. doi: 10.1002/hep.25789 PMID: 22508243

The American Journal of Pathology, Vol. 184, No. 5, May 2014

ELSEVIER

The American Journal of
PATHOLOGY
ajp.amjpathol.org

GASTROINTESTINAL, HEPATOBILIARY, AND PANCREATIC PATHOLOGY

# Mechanisms of Action of Acetaldehyde in the Up-Regulation of the Human α2(I) Collagen Gene in Hepatic Stellate Cells

## *Key Roles of Ski, SMAD3, SMAD4, and SMAD7*

Karina Reyes-Gordillo,*† Ruchi Shah,*† Jaime Arellanes-Robledo,*† Zamira Hernández-Nazara,‡ Ana Rosa Rincón-Sánchez,§ Yutaka Inagaki,¶ Marcos Rojkind,†‡ and M. Raj Lakshman*†

*From the Lipid Research Laboratory,* Veterans Affairs Medical Center, Washington, District of Columbia; the Department of Biochemistry and Molecular Medicine,† George Washington University Medical Center, Washington, District of Columbia; the Department of Clinical Investigation,‡ Walter Reed National Military Medical Center, Bethesda, Maryland; the Department of Biochemistry and Molecular Biology,§ Mount Sinai School of Medicine, New York, New York; and the Department of Regenerative Medicine,¶ Tokai University School of Medicine, Isehara, Japan*

Accepted for publication January 6, 2014.

Address correspondence to M. Raj Lakshman, Ph.D., Director of Research Laboratories, VA Medical Center, 50 Irving St., NW, Washington, DC 20422. E-mail: raj.lakshman@va.gov.

Alcohol-induced liver fibrosis and eventually cirrhosis is a leading cause of death. Acetaldehyde, the first metabolite of ethanol, up-regulates expression of the human α2(I) collagen gene (*COL1A2*). Early acetaldehyde-mediated effects involve phosphorylation and nuclear translocation of SMAD3/4—containing complexes that bind to *COL1A2* promoter to induce fibrogenesis. We used human and mouse hepatic stellate cells to elucidate the mechanisms whereby acetaldehyde up-regulates *COL1A2* by modulating the role of Ski and the expression of SMADs 3, 4, and 7. Acetaldehyde induced up-regulation of *COL1A2* by 3.5-fold, with concomitant increases in the mRNA (threefold) and protein (4.2- and 3.5-fold) levels of SMAD3 and SMAD4, respectively. It also caused a 60% decrease in SMAD7 expression. Ski, a member of the Ski/Sno oncogene family, is colocalized in the nucleus with SMAD4. Acetaldehyde induces translocation of Ski and SMAD4 to the cytoplasm, where Ski undergoes proteasomal degradation, as confirmed by the ability of the proteasomal inhibitor lactacystin to blunt up-regulation of acetaldehyde-dependent *COL1A2*, but not of the nonspecific fibronectin gene (*FN1*). We conclude that acetaldehyde up-regulates *COL1A2* by enhancing expression of the transactivators SMAD3 and SMAD4 while inhibiting the repressor SMAD7, along with promoting Ski translocation from the nucleus to cytoplasm. We speculate that drugs that prevent proteasomal degradation of repressors targeting *COL1A2* may have antifibrogenic properties. *(Am J Pathol 2014, 184: 1458–1467; http://dx.doi.org/10.1016/j.ajpath.2014.01.020)*

Alcohol-induced liver fibrosis is a multifactorial event characterized by increased collagen production as a result of up-regulation of α2(I) collagen (*COL1A2*) gene.[1] This is induced primarily by its immediate oxidation product, acetaldehyde, as well as by other events occurring during alcohol metabolism, such as changes in redox state,[2] formation of free radicals and generation of reactive oxygen species,[2–4] and depletion of antioxidant defenses and generation of aliphatic aldehydes derived from lipid peroxidation (namely, 4-hydroxy-nonenal and malonyldialdehyde).[5] Because ethanol

Supported in part by NIH grants AA-010541 and AA-009231 (M.R.L.), a grant-in aid from the Ministry of Education, Culture, Sports, Science and Technology, Japan (Y.I.), and CONACYT—Mexico National Council of Science and Technology fellowships 137122 (K.R.-G.) and 128405 and 151478 (J.A.-R.).

The opinions or assertions contained herein are the private views of the authors and are not to be construed as official or as reflecting the views of the U.S. Department of the Army or the Department of Defense.

K.R.-G. and R.S. contributed equally to this work.

M.R. is deceased.


http://dx.doi.org/10.1016/j.ajpath.2014.01.020

also increases the circulation of bacterial-derived endotoxin,[6–8] and this in turn up-regulates expression of inflammatory cytokines, the aforementioned events also play a role in the inflammatory response and therefore in fibrogenesis and complications resulting from chronic alcoholic liver disease.[7,9]

To unravel key molecular mechanisms involved in acetaldehyde-mediated up-regulation of type I collagen, we have investigated the key roles played by this ethanol metabolite in up-regulation of type I collagen genes in hepatic stellate cells (HSCs).[1] We have shown that several different transcription factors are involved in acetaldehyde-dependent up-regulation of the type I collagen genes. Although CAAT/enhancing binding protein p35C (p35C/EBPβ) is required for expression of the α1(I) collagen mRNA,[10] Sp1 and SMAD3 are essential for up-regulation of *COL1A2* gene.[11] We and others have also shown that reactive oxygen species in general,[2–4] and $H_2O_2$ in particular, play a key role in the acetaldehyde-elicited response and that $H_2O_2$ acts as a second messenger in both acetaldehyde-dependent and transforming growth factor β1 (TGF-β1)–dependent up-regulation of type I collagen genes.[2,10]

Acetaldehyde up-regulates expression of *COL1A2* gene via a *de novo* protein synthesis–independent, PI3K-dependent mechanism.[12] In addition, the early acetaldehyde-mediated effects, occurring during the first 6 to 12 hours after acetaldehyde treatment, are independent of TGF-β1.[12] However, the mechanisms whereby acetaldehyde modulates expression and activity of members of the SMAD family, including SMAD3, SMAD4, and SMAD7, leading to *COL1A2* up-regulation are not well understood. Here, we show that SMAD3 and SMAD4 are the limiting factors in *COL1A2* gene up-regulation and that this ethanol metabolite enhances expression of SMAD3 and SMAD4 at the mRNA and protein levels.

c-Ski, a homolog of v-Ski in cells and a versatile transcriptional regulator that is widely distributed in different tissues, has been reported to be a corepressor of TGF-β/SMAD signaling.[13] Binding of TGF-β to its receptor serine/threonine kinases results in the regulation of SMAD2 and SMAD3 proteins. The phosphorylated SMADs then form heteromeric complexes with a common mediator SMAD4 (co-SMAD).[14] Together, they translocate into the nucleus, where they bind to DNA and activate transcription of the target genes.[15] We further show that Ski, a member of the Ski/Sno family of oncogenes, is colocalized in the nucleus with SMAD4 and that acetaldehyde induces their cotranslocation to the cytosol, where Ski is degraded by proteasomes. We also demonstrate that inhibiting proteasomal degradation of Ski by lactacystin blunts the acetaldehyde-dependent up-regulation of *COL1A2* gene, but has no effect on expression of the nonspecific protein fibronectin.

## Materials and Methods

### Plasmids and Reagents

TGF-β1 was purchased from Roche Diagnostics (Indianapolis, IN). Lactacystin was purchased from Calbiochem–Novabiochem (Millipore, Billerica, MA). Acetaldehyde was purchased from Thermo Fisher Scientific (Waltham, MA). The construction of the −378COL1A2LUC chimeric plasmid containing the −378 to +54 region of *COL1A2* linked to the firefly luciferase gene has been described previously.[12] SMAD3, -4, and -7 expression plasmids cloned into the pcDNA3 cytomegalovirus expression vector (Life Technologies, Carlsbad, CA) have been described previously.[11,16] The cDNAs of COL1A2, fibronectin, and TGF-β1 have been described previously.[17–19] S14 ribosomal protein cDNA was obtained from ATCC (Manassas, VA). cDNA fragments of human SMAD3 (nucleotides 501 to 878) and SMAD4 (nucleotides 601 to 1050) were used to determine steady-state levels of SMAD3 and SMAD4 mRNAs. Nonspecific IgG rabbit, mouse, and goat polyclonal antibodies against Ski (sc-9140), SMAD3 (sc-101154), and SMAD4 (sc-1909), respectively, were obtained from Santa Cruz Biotechnology (Dallas, TX). Neutralizing antibody to TGF-β1 was obtained from Promega (Madison, WI).

### HHSC Isolation and Culture

Human HSCs (HHSCs) were isolated from a consenting study subject with clinically proven normal healthy liver during gastric bypass surgery for morbid obesity as described previously.[1] Informed consent in writing was obtained from the study patient, and the study protocol conformed to the ethical guidelines of the 1975 Declaration of Helsinki as reflected in a prior approval by the Institutional Review Committee. For some experiments, mouse HSCs were isolated as described previously.[20] Cells were cultured in Dulbecco's modified Eagle's medium supplemented with 10% fetal bovine serum (HyClone; Thermo Fisher Scientific, Waltham, MA) and antibiotics. Experiments were performed in triplicate, using cells obtained from at least three different patients cultured for 2 to 8 passages.

### Northern Blot Hybridization and Run-On Transcription Assay

Confluent HHSCs were placed in a serum-free medium containing glutamine, nonessential amino acids, and antibiotics. Approximately 14 hours later, acetaldehyde was added at a final concentration of 200 μmol/L. Viability of cells was estimated using the trypan blue exclusion test. In all cases, cellular viability was greater than 90%. Total RNA was extracted at 30 minutes and 1, 3, 24, and 48 hours and was processed for Northern blot hybridizations according to standard protocols.[12] Likewise, a standard protocol was used to determine rates of COL1A2, fibronectin, and TGF-β1 transcription in control and acetaldehyde-treated cells, using S14 and pBR322 DNA as controls.[11]

In some run-on transcription experiments, cells were preincubated with 30 μmol/L lactacystin for 2 hours before acetaldehyde administration; in others, cells were preincubated for 2 hours with a neutralizing antibody to TGF-β1

(Promega) or an unrelated IgG (Santa Cruz Biotechnology) at a final concentration of 5 μg/mL. To determine the effectiveness of the anti–TGF-β1 antibody, some HHSCs were also incubated with 8 ng/mL of recombinant TGF-β1 in the presence or absence of the corresponding neutralizing antibody, or an unrelated IgG, according to a protocol described previously.[21] Nuclei were isolated at 15 and 30 minutes and were used in run-on transcription assays as described previously.[12] Relative intensity of the signals was determined by laser densitometric analysis of the radiographic films. Data were corrected for loading differences, using S14 as control.

## RT-PCR Analysis

Transcript levels of SMADs 3, 4, and 7 in HHSCs were measured using a quantitative RT-PCR technique (RT-qPCR). Experiments were performed as described previously.[22] Primer sequences for qPCR amplification were as follows: SMAD3 mRNA , forward 5′-GAGGGCAGGCTTGGGGAAAATG-3′ and reverse 5′-GGGAGGGTGCCGGTGGTGTAATAC-3′; SMAD4 mRNA, forward 5′-AAAGGTGAAGGTGATGTTTGGGTC-3′ and reverse 5′-CTGGAGCTATTCCACCTACTGATCC-3′; SMAD7 mRNA, forward 5′-CGAGACCCTTCTCACTCCTG-3′ and reverse 5′-GCATCCTTGGTTAGGGTCAA-3′; and GAPDH mRNA, forward 5′-GGCCTCCAAGGAGTAAGACC-3′ and reverse 5′-CTGTGAGGAGGGGAGATTTCA-3′. All reagents were purchased from Life Technologies. Relative gene expression was calculated as

$$2^{-\Delta Ct}\left[C_{T(\text{target})} - C_{T(\text{housekeeping})}\right]_{\text{time } X} - \left[C_{T(\text{target})} - C_{T(\text{housekeeping})}\right]_{\text{time } 0.} \quad (1)$$

## Western Blot Analysis

Total, nuclear, and cytosolic extracts were prepared from control and acetaldehyde-treated HHSCs as described previously.[1,12] In some experiments, HHSCs were treated with 8 ng/mL recombinant TGF-β1; in other experiments, cells were preincubated for 60 minutes with 30 μmol/L lactacystin before administration of acetaldehyde or TGF-β1. Total extracts (20 μg) were separated by SDS-PAGE on 10% gels, transferred onto a nitrocellulose membrane, and probed with SMAD3 or SMAD4 goat antibodies (1:1000; Santa Cruz Biotechnology), followed by incubation with horseradish peroxidase–conjugated rabbit anti-goat IgG (1:5000; Santa Cruz Biotechnology). Nuclear and cytosolic extracts were separated by SDS-PAGE on 4% to 12% gels, transferred onto polyvinylidene difluoride membranes, and probed with Ski rabbit antibody (1:1000; Santa Cruz Biotechnology), followed by incubation with horseradish peroxidase–conjugated chicken anti-rabbit secondary antibody (1:2000; Santa Cruz Biotechnology). Proteins were detected with a NEN Life Science Products Renaissance enhanced chemiluminescence system (PerkinElmer, Waltham, MA), according to the manufacturer's recommendations.

## Coimmunoprecipitation of Ski with SMAD4 and 20S Proteasome

The coimmunoprecipitation experiment was performed as described previously.[23] In brief, SMAD4 was immunoprecipitated with a SMAD4 antibody (Santa Cruz Biotechnology) bound to protein L-agarose beads (Santa Cruz Biotechnology), and the amount of Ski coimmunoprecipitated with SMAD4 was quantified by Western analysis using Ski antibody (1:1000; Santa Cruz Biotechnology).

## Cell Transfections

Conditions for the preparation and transfection of plasmids into HHSCs by the calcium phosphate procedure have been described previously.[12,16] HHSCs were treated with 10% glycerol for 90 seconds, at 6 hours after transfection, and then were placed in medium containing 0.1% fetal bovine serum. Twelve hours later, acetaldehyde was added at the final concentration of 200 μmol/L, unless otherwise indicated. For some experiments, 8 ng/mL TGF-β1 (unless otherwise indicated) was added, alone or in combination with acetaldehyde. Cells were procured at 36 hours after the addition of acetaldehyde and were used to determine luciferase activity as described previously.

In some experiments, cells were preincubated for 60 minutes with 30 μmol/L lactacystin before administration of acetaldehyde. Transcriptional activity of acetaldehyde of the chimeric constructs was normalized against cotransfected pSV2CAT. Transfections were performed multiple times and in duplicate. For some experiments, HHSCs were cotransfected with 7.0 μg of the −378COL1A2LUC reporter construct and 2.5 μg of a SMAD4 vector, followed by treatment with acetaldehyde using the conditions described above. For other experiments, HHSCs were cotransfected with 7.0

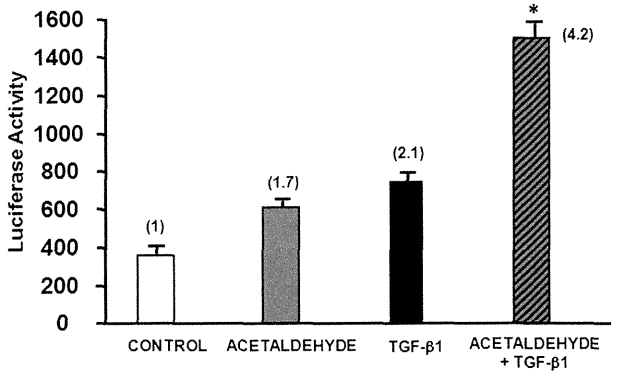


**Figure 1** Effect of acetaldehyde, TGF-β1, or the two in combination on the expression of a reporter vector driven by the −378COL1A2 promoter in HSCs. First, HHSCs were transfected with the reporter vector. Next, 12 hours later, cells were incubated with either 100 μmol/L acetaldehyde, 4 ng/mL TGF-β1, or both. Then, 36 hours later, cells were harvested and luciferase activity was determined. Cells treated with the combination of acetaldehyde and TGF-β1 showed a 4.2-fold increase in reporter activity. Controls were transfected cells without treatment. Data are expressed as means ± SEM. *$P < 0.05$ versus control.

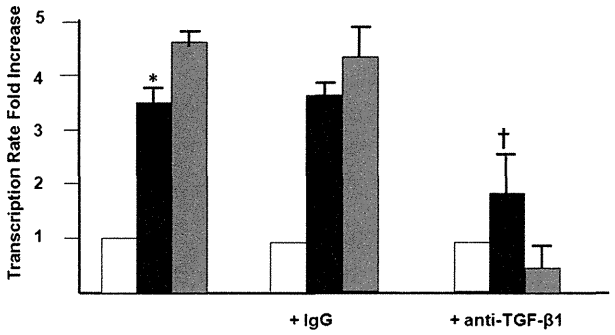


**Figure 2** TGF-β1 is involved in late acetaldehyde-dependent up-regulation of *COL1A2*. Run-on transcription assays of control (white bars; untreated cells in serum-free medium) and acetaldehyde-treated (black bars) HHSCs for 24 hours in the presence or absence of a nonspecific IgG or a neutralizing antibody to TGF-β1 (gray bars; anti—TGF-β1). As a control for these experiments, some HSCs were treated with 2 ng/mL of TGF-β1 in the absence or presence of the neutralizing antibody to the cytokine. *COL1A2* gene transcription was up-regulated 3.5-fold by acetaldehyde, whereas the neutralizing antibody to TGF-β1 strongly inhibited *COL1A2* gene transcription in cells treated with acetaldehyde by 60%. The nonspecific immunoglobulin had no effect. Data are expressed as means ± SEM. $^{*}P < 0.05$ versus control. $^{\dagger}P < 0.05$ versus acetaldehyde-treated cells.

μg of the −378COL1A2LUC reporter construct and 2.5 μg of vectors overexpressing SMAD3, SMAD4, both SMAD3 and SMAD4, or SMAD7, followed by treatment with acetaldehyde using the conditions described above.

### Immunostaining

Mouse HSCs plated on coverslips were fixed with 4% paraformaldehyde for 10 minutes, permeabilized with −20°C cold acetone for 30 minutes, rinsed with PBS, and blocked with 3% bovine serum albumin—PBS for 1 hour. After blocking, cells were incubated overnight with a goat polyclonal antibody against Ski (1:10) and rabbit polyclonal antibody against SMAD4 (1:10), followed by the appropriate fluorophore-conjugated secondary antibody for 1 hour (1:300); between acetaldehyde procedures, coverslips were washed with 0.1% Tween 20—PBS and mounted on glass slides with Gel-Mount medium (BioMeda, Foster City, CA). Images were captured using an AX70 light microscope (Olympus, Tokyo, Japan) and were processed with Photoshop software version 5.0.2 (Adobe Systems, San Jose, CA).

### Statistical Analysis

Statistical differences between experimental groups were analyzed by Student's *t*-test (normally distributed data with equal variances) or *U* test (normally distributed data with different variances). All *P* values of ≤0.05 were considered significant. Data represent three to six independent experiments using HHSCs obtained from a single patient. Data are expressed as means ± SEM.

## Results

### Acetaldehyde and TGF-β1 Have an Additive Effect on Expression of a Reporter Vector Driven by the Acetaldehyde-Responsive Element −378COL1A2LUC

Because TGF-β1 also induced expression of SMADs 3 and 4, and given that the acetaldehyde and TGF-β1 responsive elements are localized in the same region of the *COL1A2* promoter, it was important to determine whether acetaldehyde and TGF-β1 up-regulation of *COL1A2* gene expression is additive or synergistic. To this end, we transfected HSCs with the −378COL1A2LUC reporter vector and treated these cells with 100 μmol/L acetaldehyde, 4 ng/mL TGF-β1, or both. It is important to note that the doses used were half of those normally used in our previous experiments,[12] and we therefore expected a weaker individual response. Neither acetaldehyde nor TGF-β1 alone was sufficient to up-regulate expression of the *COL1A2* reporter vector to previously observed levels (Figure 1).[12] However, cells treated with the combination of acetaldehyde and TGF-β1 responded with a 4.2-fold increase in reporter activity ($P < 0.05$), indicating that acetaldehyde and TGF-β1 have an additive stimulatory effect on the activity of *COL1A2* reporter vector.

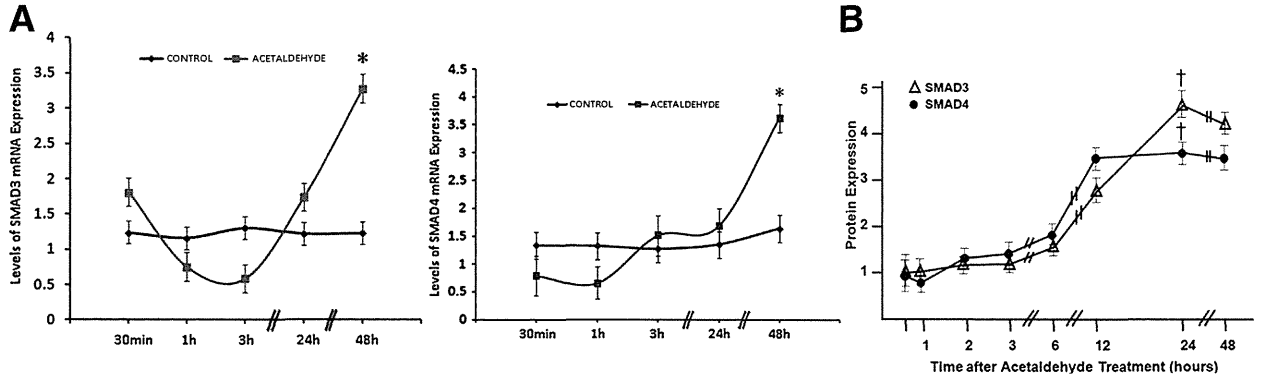


**Figure 3** Increase in SMAD3 and SMAD4 mRNA and protein is delayed after acetaldehyde treatment. **A:** Time-course analysis of SMAD3 and SMAD4 mRNA expression levels after acetaldehyde treatment. Total RNA obtained from HHSCs cultured in the absence or presence of 200 μmol/L acetaldehyde for times ranging from 30 minutes to 48 hours was used to determine steady-state levels of SMAD3 and SMAD4 mRNAs by using RT-PCR analysis. **B:** Replica dishes were used to obtain cell extracts and to determine levels of SMAD3 and SMAD4 protein by Western analysis. Data are expressed as means ± SEM. $^{*}P < 0.05$ versus control (**A**); $^{\dagger}P < 0.05$ versus 30-minute time point (**B**).

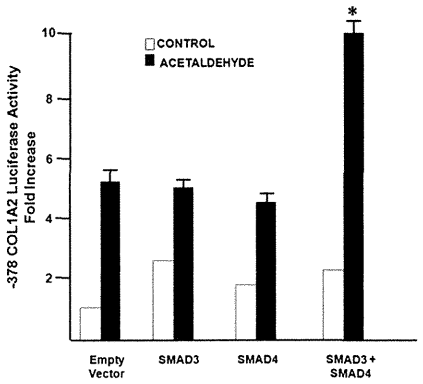


**Figure 4** SMAD3 and SMAD4 are limiting factors for acetaldehyde-mediated *COL1A2* up-regulation in HSCs. Effect of acetaldehyde on luciferase activity of HSCs transiently cotransfected with 7 μg −378COL1A2LUC reporter vector and either a control empty cytomegalovirus vector or 2.5 μg expression vectors for SMAD3 or SMAD4. At 12 hours after transfection, cells were treated with 200 μmol/L acetaldehyde for 36 hours. Cells were harvested and used to measure luciferase activity. Up-regulation of either SMAD3 or SMAD4 alone does not significantly enhance reporter activity induced by acetaldehyde; however, in HHSCs cotransfected with both the reporter vector and the two vectors expressing SMAD3 and SMAD4, reporter activity increased twofold, compared with that induced by acetaldehyde alone or cells expressing either SMAD3 or SMAD4. Data are expressed as means ± SEM. $*P < 0.05$.

## The Late Acetaldehyde-Dependent Up-Regulation of COL1A2 Transcription Is Mediated by TGF-β1

We have shown that acetaldehyde is directly responsible for the early expression of α2(I) collagen mRNA and for changes in cell signaling occurring early (before 6 to 12 hours). However, the late events appear to be associated with acetaldehyde-induced expression of TGF-β1. To test this possibility, we measured the late acetaldehyde-dependent transcription of *COL1A2* gene in the presence of a TGF-β1 neutralizing antibody. We used a nonspecific immunoglobulin as a control for these experiments. Transcription of *COL1A2* was up-regulated 3.5-fold by acetaldehyde ($P < 0.05$) (Figure 2). Whereas the neutralizing antibody to TGF-β1 strongly inhibited *COL1A2* gene transcription of cells treated with acetaldehyde by 60% ($P < 0.05$), the nonspecific immunoglobulin had no effect.

## Acetaldehyde Induces the Late Expression of SMAD3 and SMAD4 mRNAs in HSCs

We have already shown that acetaldehyde induces formation of SMAD3/4 complexes that bind to the *COL1A2* promoter and phosphorylates SMAD3.[12] Thus, we considered it important to investigate whether acetaldehyde induces expression of SMADs 3 and 4 and whether this is an early event directly induced by acetaldehyde per se or a late event resulting from up-regulation of TGF-β1. We determined the time course of expression of SMAD3 and SMAD4 mRNA and protein in HHSCs incubated with acetaldehyde. Acetaldehyde up-regulated the mRNA expression of SMADs 3 and 4 approximately threefold ($P < 0.05$ for both) and up-regulated SMAD3 protein expression 4.2-fold ($P < 0.05$) and SMAD4 protein expression 3.5-fold ($P < 0.05$) (Figure 3). This effect was observed by approximately 24 hours after incubation with acetaldehyde and lasted up to 48 hours, a time period that coincided with acetaldehyde-induced up-regulation of TGF-β1 mRNA expression.

## Both SMAD3 and SMAD4 Are Limiting Factors in Acetaldehyde-Elicited Up-Regulation of *COL1A2*

To further test the requirement of SMAD3 and SMAD4 in acetaldehyde-elicited up-regulation of *COL1A2*, we cotransfected HHSCs with the −378COL1A2LUC reporter vector and a vector that overexpressed either SMAD3 or SMAD4 and determined the reporter activity in cells treated with or without 200 μmol/L acetaldehyde. Overexpression of either SMAD3 or SMAD4 alone did not significantly enhance reporter activity induced by acetaldehyde. However, when HHSCs were cotransfected with the reporter vector and

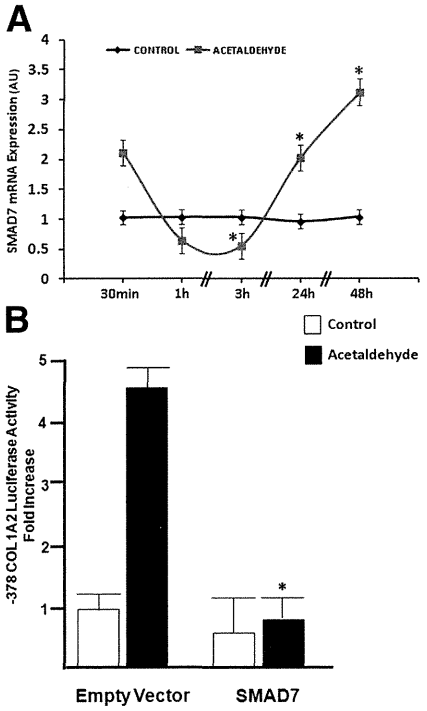


**Figure 5** Acetaldehyde modulates SMAD7 expression. **A:** Total RNA was obtained from HHSCs cultured in the absence or presence of 200 μmol/L acetaldehyde for times ranging from 30 minutes to 48 hours. Acetaldehyde down-regulates the expression of SMAD7 mRNA in a time-dependent manner, reaching the maximum down-regulation of 60% after 3 hours, relative to the value at 30 minutes, after which time expression increases steadily and reaches values threefold above basal levels by 48 hours. SMAD7 mRNA expression levels were corrected for differences in loading using *GAPDH* as a housekeeping gene. $*P < 0.05$ versus control. **B:** HHSCs were transiently cotransfected with the −378COL1A2 reporter plasmid and a cytomegalovirus-driven SMAD7 expression vector. At 12 hours after transfection, cells were treated with 200 μmol/L acetaldehyde for 36 hours. Cells were harvested and used to measure luciferase activity. Acetaldehyde failed to up-regulate the expression of *COL1A2* reporter vector in HHSCs cotransfected with a vector overexpressing SMAD7 and the −378COL1A2LUC reporter vector. Data are expressed as means ± SEM. $*P < 0.05$ versus acetaldehyde-treated empty vector. AU, arbitrary units.